A posteriori error estimates for primal hybrid finite element methods

Victor B. Oliari[1], Paulo Rafael Bösing[2], Denise de Siqueira[3], Philippe R. B. Devloo[1]

[1]*Dept. of Civil Engineering, State University of Campinas (UNICAMP)*
Street Saturnino de Brito 224, 13083-889, Campinas/São Paulo, Brazil
v104268@dac.unicamp.br, phil@fec.unicamp.br
[2]*Dept. of Mathematics, Federal University of Fronteira Sul (UFFS)*
Rodovia SC 484 - Km 02, 89815-899, Chapecó/SC, Brazil
paulo.bosing@uffs.edu.br
[3]*Dept. of Mathematics, Federal University of Technology – Paraná (UTFPR-CT)*
Av. Sete de Setembro, 80230-901, Curitiba/Paraná, Brazil
denisesiqueira@utfpr.edu.br

Abstract.

We present new fully computable a posteriori error estimates for the primal hybrid finite element methods based on equilibrated flux and potential reconstructions. The reconstructed potential is obtained from a local L^2 orthogonal projection of the gradient of the numerical solution, with a boundary continuous restriction that comes from a smoothing process applied to the trace of the numerical solution over the mesh skeleton. The equilibrated flux is the solution of a local mixed form problem with a Neumann boundary condition given by the Lagrange multiplier of the hybrid finite element method solution.

To establish the a posteriori estimates we divide the error into conforming and non-conforming parts. For the former one, a slight modification of the a posteriori error estimate proposed by Vohralík [1] is applied, whilst the latter is bounded by the difference of the gradient of the numerical solution and the reconstructed potential.

Numerical results performed in the environment PZ Devloo [2], show the efficiency of this strategy when it is applied for some test model problems.

Keywords: FEM, Primal Hybrid, A Posteriori Error Estimate

1 Introduction

From the Generalized Prager–Synge (GPS) identity establish in the recent paper Cai et al. [3], we propose and evaluate a new a posteriori error estimator for primal hybrid finite element methods applied to the Poisson problem. The GPS identity extends the well-known Prager and Synge [4] (PS) identity (see also Bertrand and Boffi [5]), which is valid for $H^1(\Omega)$, for discontinuous functions and can be applied to provide a way to get guaranteed upper bounds for the error associated to non-conforming methods. Usually, the PS identity for H^1-conforming formulation gives a posteriori estimate since an equilibrated flux is defined. Several works follow this direction, see for example Braess et al. [6]. For $H(div, \Omega)$-conforming formulation, it is necessary to obtain a reconstructed potential to establish an a posteriori estimate, as in Cai et al. [7]. In the primal hybrid formulation, where the solution is neither $H^1(\Omega)$ nor $H(div, \Omega)$-conforming, it is necessary to obtain the equilibrated flux and the reconstructed potential simultaneously, as in Pencheva et al. [8].

In the current work, the reconstructed potential is obtained as a local L^2 orthogonal projection of the gradient of the numerical solution, with smooth boundary conditions that will ensure a global regularity. The boundary conditions are continuous function obtained from the numerical solution. To obtain the equilibrated flux, the local mixed problems are solved using the Lagrange multiplier of the numerical solution as the Neumann boundary conditions. This procedure ensures that the reconstructed flux is equilibrated and is in $H(div, \Omega)$.

The work is organized as follows: the basic notation, the model problem and its discrete version are introduced in the next section. The a posteriori estimates, the potential and flux reconstruction procedures are presented

in Section 3. Finally, Section 4 evaluates the proposed error estimator for a problem with smooth solution and a singularity problem.

2 Notation and preliminaries

Consider the following model problem in a polygonal domain $\Omega \subset \mathbf{R}^2$:

$$\left\{\begin{array}{rcll} \nabla \cdot (-\mathbf{K}\nabla u) & = & f, & \text{in } \Omega \\ u & = & g_D, & \text{on } \partial\Omega_D \\ -\boldsymbol{K}\boldsymbol{\nabla} u \cdot \boldsymbol{n} & = & g_N, & \text{on } \partial\Omega_N \end{array}\right. , \tag{1}$$

where $f \in L^2(\Omega)$, $g_D \in \mathcal{C}(\Omega_D)$, $g_N \in L^2(\partial\Omega_N)$ and $\mathbf{K}$ is a uniformly bounded symmetric positive definite tensor. The boundary $\partial\Omega$ is divided into the disjoint parts $\partial\Omega_D$ and $\partial\Omega_N$, such that, $\partial\Omega = \partial\bar{\Omega}_D \cup \partial\bar{\Omega}_N$ and $\partial\Omega_D$ is non-empty set.

Let $\mathbb{T} = \{\mathcal{T}_h\}$ be a family of shape-regular triangulations of a domain $\Omega \subset \mathbb{R}^2$. The elements $K \in \mathcal{T}_h$ are open, convex and pairwise disjoint, such that, $\overline{\Omega} = \bigcup_{K\in\mathcal{T}_h} \overline{K}$. Associated to $\mathcal{T}_h \in \mathbb{T}$ there is a piecewise constant function $h_{\mathcal{T}_h}$ defined by: $h_{\mathcal{T}_h|K} = h_K := \text{diam}(K), \quad K \in \mathcal{T}_h$. The index h refers to the maximum of $h_K, K \in \mathcal{T}_h$. Let $\mathcal{E}_h$ be the set of all edges E of all elements in $\mathcal{T}_h$. It is divided into two subsets: $\mathring{\mathcal{E}}_h = \{E \in \mathcal{E}_h : \ E \subset \Omega\}$ and $\mathcal{E}_\partial = \{E \in \mathcal{E}_h : \ E \subset \partial\Omega\}$.

For $\omega \subset \Omega$, the scalar Sobolev space $H^\alpha(\omega)$, of real order (or index) α, is equiped with the usual inner product, norm and semi-norm $(\cdot,\cdot)_{\alpha,\omega}$, $\|\cdot\|_{\alpha,\omega}$, and $|\cdot|_{\alpha,\omega}$, respectively. In particular, for $\alpha = 0$, the notation $\|\cdot\|_\omega$ and $(\cdot,\cdot)_\omega$ is adopted instead of $\|\cdot\|_{0,\omega}$ and $(\cdot,\cdot)_{0,\omega}$, respectively. Similarly, for any $E \in \mathcal{E}_h$, denote by $\langle\cdot,\cdot\rangle_E$ and $\|\cdot\|_E$ the inner product and the induced norm in the space $L^2(E)$, respectively. The subscript ω is dropped when $\omega = \Omega$.

The space of vector functions with square-integrable weak divergences will be denoted by $H(div,\Omega)$, and $H^\alpha(\mathcal{T}_h)$ is the space of piecewise Sobolev H^α-functions, $H^\alpha(\mathcal{T}_h) = \{v \in L^2(\Omega) : v_{|K} \in H^\alpha(K), \forall\ K \in \mathcal{T}_h\}$. Also, the following spaces are required,

$$\Lambda(\mathcal{E}_h) = \left\{\mu \in H^{-1/2}(\mathcal{E}_h); \mu = \boldsymbol{\sigma}\cdot\boldsymbol{n}^K_{|\partial K},\ \boldsymbol{\sigma} \in H(div,\Omega),\ \ \forall\ K \in \mathcal{T}_h\right\},$$
$$\Lambda_{0,N}(\mathcal{E}_h) = \left\{\mu \in \Lambda(\mathcal{E}_h); \mu_{|\partial\Omega_N} = 0\right\}, \quad \text{and } \ \Lambda_{g,N}(\mathcal{E}_h) = \left\{\mu \in \Lambda(\mathcal{E}_h); \mu_{|\partial\Omega_N} = g_N\right\}.$$

Finally, any differential operator defined over piecewise Sobolev spaces will be indicated with the same notation used for the classic Sobolev spaces. The argument indicates that it should be taken piecewise.

For a given element $K \in \mathcal{T}_h$ we denote $\boldsymbol{n}^K$ the unity normal vector that points outward K, and by $\boldsymbol{n}$ the unity normal vector on $\partial\Omega$. Additionally, there is an associated element $\hat{K}$ and an invertible geometric diffeomorfism $F_K : \hat{K} \to K$, transforming $\hat{K}$ into K (analogous for a face $E \in \mathcal{E}_h$). For this paper, consider the quadrilateral $\hat{K} = [-1,\ 1] \times [-1,\ 1]$ and linear $\hat{E} = [-1,\ 1]$ elements.

We denote by $\mathbb{Q}_{k_1,k_2}(\hat{K})$ the polynomial of maximum degree $k_i, i = 1, 2$, in each variable over the element $\hat{K}$ and $\mathbb{Q}_k(\hat{K}) = \mathbb{Q}_{k,k}(\hat{K})$. Then, the following finite approximation space are defined, $Y_k = \{\mu \in \Lambda_{g,N}(\mathcal{E}_h) : \mu|_E \in \mathbb{Q}_k(E),\ \forall E \in \mathcal{E}_h\}$, and for a given natural $n \geq 1$, the enriched polynomial space is defined by $U_k^{+n} = \left\{v \in H^1(\mathcal{T}_h) : v|_K \in \mathbb{Q}_{k+n}(K),\ \forall K \in \mathcal{T}_h\right\} \subset H^1(\mathcal{T}_h)$.

The standard finite element approximation for the problem (1) consist of construct a finite subspace of $H^1(\Omega)$ with functions which are continuous at the inter-element boundaries. As for broken space $H^1(\mathcal{T}_h)$, the constraint of inter-element continuity has been removed, the continuity is imposed introducing the Lagrange multiplier among the inter-element, for a complete description of the method see Raviart and Thomas [9].

The discrete primal hybrid formulation can be read as: Find $(\lambda_h, u_h) \in Y_k \times U_k^{+n}$, such that,

$$\sum_{K\in\mathcal{T}_h} \langle\mu_h, u_h\rangle_{\partial K} = \sum_{K\in\mathcal{T}_h} \langle\mu_h, g_D\rangle_{\partial K\cap\partial\Omega_D}, \qquad \forall\mu_h, \in Y_k \cap \Lambda_{0,N}(\mathcal{E}_h) \tag{2}$$

$$\sum_{K\in\mathcal{T}_h} [(\boldsymbol{K}\nabla u_h, \nabla v_h)_K + \langle\,\lambda_h,\ v_h\rangle_{\partial K}] = \sum_{K\in\mathcal{T}_h} (f, v_h)_K,\ \forall v_h \in U_k^{+n}. \tag{3}$$

As the approximate solutions u_h given by the primal hybrid formulation (2)-(3) is not in $H^1_{g_D}(\Omega)$ and $-\mathbf{K}\nabla u_h \notin \mathbf{H}(\text{div}, \Omega)$, we can introduce a "correction" for this phenomenon using the concept of "reconstructed flux" and "reconstructed potential", that are introduced in the next section.

3 A posteriori error estimates

In many numerical solutions of practical problems the accuracy of the numerical approximation is deteriorated by local singularities that can be arisen, for example, from re-entrant corners, interior or boundary layers or change of the boundary condition. As mentioned by Verfürth [10], an alternative can be to refine the approximation solution near the critical regions, but how to identify those regions and how to obtain a good balance between the refined and unrefined regions such that the accuracy is optimal? In this case, a posteriori error estimation is useful for efficient error control of the numerical simulations, in practical problems where the real solution is unknown. The approach adopt in the current work is based on Prager-Synge Theorem (see Prager and Synge [4] and Bertrand and Boffi [5]) which provides an orthogonality relationship that leads to an upper bound for the unknown exact error.

On Prager-Synge Theorem, given $u \in H^1_D(\Omega)$ a solution of (1), it holds for all $w \in H^1_D(\Omega)$ and $\boldsymbol{\sigma} \in \Sigma_f(\Omega) = \{\boldsymbol{\sigma} \in H(\text{div}, \Omega) : \nabla \cdot \boldsymbol{\sigma} = f \text{ in } \Omega, \boldsymbol{\sigma} \cdot \mathbf{n}|_{\partial\Omega_N} = g_N\}$, that,

$$\|\boldsymbol{K}^{-1/2}\boldsymbol{\sigma} + \boldsymbol{K}^{1/2}\nabla w)\|^2 = \|\boldsymbol{K}^{1/2}\nabla(u-w)\|^2 + \|\boldsymbol{K}^{-1/2}\boldsymbol{\sigma} + \boldsymbol{K}^{1/2}\nabla u\|^2.$$

The variable $w \in H^1_D(\Omega)$ is the reconstructed potential and $\boldsymbol{\sigma} \in \Sigma_f(\Omega)$ is the *reconstructed flux*, also known as *equilibrated flux*.

Cai et al. [3] proposed a Generalized Prager-Synge identity applicable to broken Sobolev space $H^1(\mathcal{T}_h)$ in sense that, given $u \in H^1_D(\Omega)$ be the solution of (1), then for all $w \in H^1(\mathcal{T}_h)$,

$$\|\boldsymbol{K}^{1/2}\boldsymbol{\nabla}_h(u-w)\|^2 = \inf_{\boldsymbol{\tau}\in\Sigma_f(\Omega)} \|\boldsymbol{K}^{-1/2}\boldsymbol{\tau} + \boldsymbol{K}^{1/2}\boldsymbol{\nabla}_h w\|^2 + \inf_{v\in H^1_D(\Omega)} \|\boldsymbol{K}^{1/2}\boldsymbol{\nabla}_h(v-w)\|^2.$$

As a consequence of the GPS identity, it is possible to derive a following reliable a posteriori error estimation in the energy norm for the potential, which are free of an indeterminated constant. A similar a posteriori error estimate was proposed to a wide class of finite element methods in Pencheva et al. [8]. However, the strategy proposed in this work is different since it is based on the Helmholtz decomposition, which is also the key ingredient in the establishment of GPS identity.

Theorem 1 *Let $\Omega \subset \mathbf{R}^2$, u be the weak solution of model problem (1), and $u_h \in H^1(\mathcal{T}_h)$ be the solution of the hybrid primal approximation (2)-(3), then it holds that,*

$$\|\boldsymbol{K}^{1/2}\boldsymbol{\nabla}_h(u-u_h)\|^2 \leq \sum_{K\in\mathcal{T}_h} \left(\eta_{K,R} + \eta_{K,F}\right)^2 + \sum_{K\in\mathcal{T}_h} \eta_{K,NC},$$

where

$$\eta_{K,R} = \frac{C_P^{1/2} h_K}{C^{1/2}_{\boldsymbol{K},K}} \|f - f_k\|_K, \quad \eta_{K,F} = \|\boldsymbol{K}^{-1/2}(\mathbf{t}_h + \boldsymbol{K}\boldsymbol{\nabla} u_h)\|_K, \text{ and } \eta_{K,NC} = \|\boldsymbol{K}^{1/2}\boldsymbol{\nabla}_h(s_h - u_h)\|^2_K.$$

Here, $C_P = \frac{1}{\pi^2}$(see Vohralík [11] and references therein) is the constant from the Poincaré inequality, $C_{\boldsymbol{K},K}$ is the smallest eigenvalue of $\boldsymbol{K}$ on K, and s_h and $\mathbf{t}_h$ are the reconstructed potential and the reconstructed equilibrated flux, respectively.

Observe that the a posteriori error estimator given by Theorem 1, is viable only if the reconstructed functions s_h and $\mathbf{t}_h$ can be reconstructed using only local computations.

The current work, propose to construct s_h and $\mathbf{t}_h$ as follows: The potential s_h is based on Ainsworth and Ma [12] and is obtained using two steps: a) a smoothing procedure; and b) solving a local Dirichlet boundary problem. To obtain an equilibrated flux, a local mixed problem is solved using the Lagrange multiplier λ_h, obtained from the primal hybrid approximation (2)-(3), as a Neumann boundary condition. The procedures are described below.

Potential Reconstructed Once we have the numerical solution u_h of formulation (2)-(3), the potential reconstruct s_h is build up in next two steps:

a) Inter-element smoothing procedure: For all $E \in \mathring{\mathcal{E}}_h$ such that $E = \partial K^i \cap \partial K^j$, with $K^i,\ K^j \in \mathcal{T}_h$, set the function $\gamma \in Y_k$ such that $\gamma|_E$ satisfying

$$\langle \frac{1}{2}(\omega(K^i) u_h^{K^i}{}_{|_E} + \omega(K^j) u_h^{K^j}{}_{|_E}) - \gamma, v\rangle_E = 0, \quad \forall\ v \in \mathbb{Q}_k(E)$$

where $u_h^K := u_h|_K$ and $\omega(K^i)$ is the largest eigenvalue of $\boldsymbol{K}$ on K^i. For $E \subset \partial\Omega_D$, we set $\gamma|_E$ as the orthogonal projection of g_D over $\mathbb{Q}_k(E)$. For $\mathbf{x}_n$ a vertex of the partition $\mathcal{T}_h$, we set the pach $\mathcal{T}(\mathbf{x}_n) = \{E \in \mathcal{E}_h;\ \boldsymbol{x}_n \in \bar{E}\}$, we update the values

$$\gamma(\mathbf{x}_n) \leftarrow \frac{1}{\omega_n} \sum_{E \in \mathcal{T}(\mathbf{x}_n)} \gamma|_E(\mathbf{x}_n),$$

with ω_n being the cardinality of $\mathcal{T}(\mathbf{x}_n)$.

b) Solving Dirichlet local problems: Given $\gamma \in Y_k$ the potentials $s_h^K = s_h|_K$ are obtained by solving primal finite element formulation of local problems in K using γ to set the boundary data. Namely, find $s_h^K \in \mathbb{Q}_{k+n}(K)$, such that,

$$\begin{aligned}(\boldsymbol{K}\nabla s_h^K, \nabla v_h)_K &= (\boldsymbol{K}\nabla u_h^K, \nabla v_h)_K, \quad \forall\ v_h \in \mathbb{Q}_{k+n}(K) \cap H_0^1(K)\\ s_h^K &= \gamma \quad \text{on} \quad \partial K.\end{aligned}$$

Note that although s_h it is locally defined as an orthogonal projection, we obtain a global smoothness.

Equilibrated flux To define the procedure for a equilibrated flux from the numerical solution u_h some definitions are necessary. Consider the finite approximation spaces over the master element $\hat{K}$: $\mathbf{M}_k^{+n}(\hat{K}) = \mathbf{Q}_k^{+n}(\hat{K}) = \mathbb{Q}_{k+n+1,k}(\hat{K}) \times \mathbb{Q}_{k,k+n+1}(\hat{K})$ and $W_{k+n}(\hat{K}) = \mathbb{Q}_{k+n}(\hat{K})$. It follows that those spaces are divergence-compatible, in sense that, $\boldsymbol{\nabla}\cdot\mathbf{M}_k^{+n}(\hat{K}) = W_{k+n}(\hat{K})$. Furthermore, $\mathbf{M}_k^{+n}(\hat{K}) \times W_{k+n}(\hat{K}) \subset H(\text{div}, \hat{K}) \times L^2(\hat{K})$. For more details about divergence compatible FE spaces see Farias et al. [13].

The equilibrated flux reconstruction $\boldsymbol{t}_h \in H(\text{div}; \Omega)$, is defined as $\boldsymbol{t}_h|_K = \boldsymbol{t}_h^K \quad \forall\ K \in \mathcal{T}_h$, where $\boldsymbol{t}_h^K$ is the (component) solution of local mixed form problem: Find $(\boldsymbol{t}_h^K, p_h^K) \in \mathbf{M}_k^{+n}(K) \times W_{k+n}(K)$, such that,

$$(\boldsymbol{K}^{-1}\boldsymbol{t}_h^K, \boldsymbol{v}_h)_K - (p_h^K, \nabla\cdot\boldsymbol{v}_h)_K = 0, \qquad \forall\ \boldsymbol{v}_h \in \mathbf{M}_k^{+n}(K) \cap H_{0,N}(\text{div}; K) \tag{4}$$

$$-(\nabla\cdot\boldsymbol{t}_h^K, w_h)_K = -(f, w_h)_K, \quad \forall\, w_h \in W_{k+n}(K) \tag{5}$$

$$\boldsymbol{t}_h^K \cdot \mathbf{n}^K = \lambda_h \quad \text{on } \partial K \tag{6}$$

where $H_{0,N}(\text{div}; K) = \{\mathbf{v} \in H(div, K) / \mathbf{v}\cdot\boldsymbol{n}_{|\partial K \cup \partial\Omega_N} = 0\}$ and the Neumann boundary condition λ_h is the Lagrange multiplier of the numerical solution of (2)-(3).

4 Numerical Results

The quality of a posteriori error estimation is described by the effectivity index, which is the quotient of the error estimate by the true error norm. That is,

$$I_e = \frac{\text{Estimated Error}}{\text{Exact Error}} = \frac{\left(\sum_{K\in\mathcal{T}_h} \left(\eta_{K,R} + \eta_{K,F}\right)^2 + \sum_{K\in\mathcal{T}_h} \eta_{K,NC}\right)^{1/2}}{\|\boldsymbol{K}^{1/2}\nabla(u - u_h)\|},$$

is expected that the effectivity index goes to one as the mesh size h goes to zero.

In order to evaluate the proposed error estimator, two problems are simulated: one with a smooth solution over a quadrilateral domain, and the other with a strong singularity at the origin over a L-shaped domain. For both simulations, only quadrilateral finite-elements are used, the diffusion tensor $\boldsymbol{K}$ is the identity, and $\partial\Omega_D = \partial\Omega$.

Problem with smooth solution: We solve the boundary value problem (1) in $\Omega = [0,\ 1]^2$, with f and g_D being chosen so that the exact solution is the function $u(x,\ y) = \sin(\pi\, x)\sin(\pi\, y)$.

The primal hybrid formulation (2)-(3) was performed with the approximation spaces $U_k^{+n} \times Y_k$ for $k = 1, n = 3$. Multiple partitions are ran $\mathbb{T} = \{\mathcal{T}_h\}$, which are obtained by uniformly refining Ω, for $h = \{1/4, 1/8, 1/16, 1/32\}$. The progression of the exact and estimated errors are shown on the left side of Fig. 1 along with the effectivity index on the right. The proposed estimated error has been shown to decrease with the same rate as the exact error as the mesh is further refined.

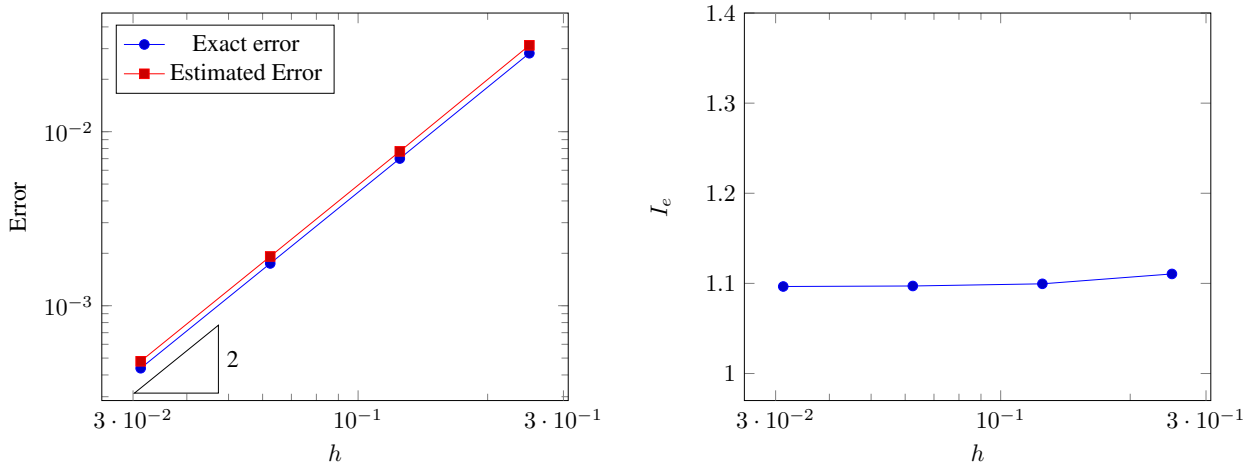

Figure 1. Smooth problem: on the left side, the histories of convergence of the exact error (blue line) and the estimator error (red line). On the right side the effectivity index I_e. The space configuration is $k = 1$, $n = 3$ and $h = \frac{1}{2^j}$, with $j = 1, \cdots 4$.

The errors over each element are shown in Fig. 2, where the exact error per element is shown on the left side and the local effectivity index, on the right side. The space configuration is $k = 1, n = 3$ and the element's diameter $h = 1/8$.

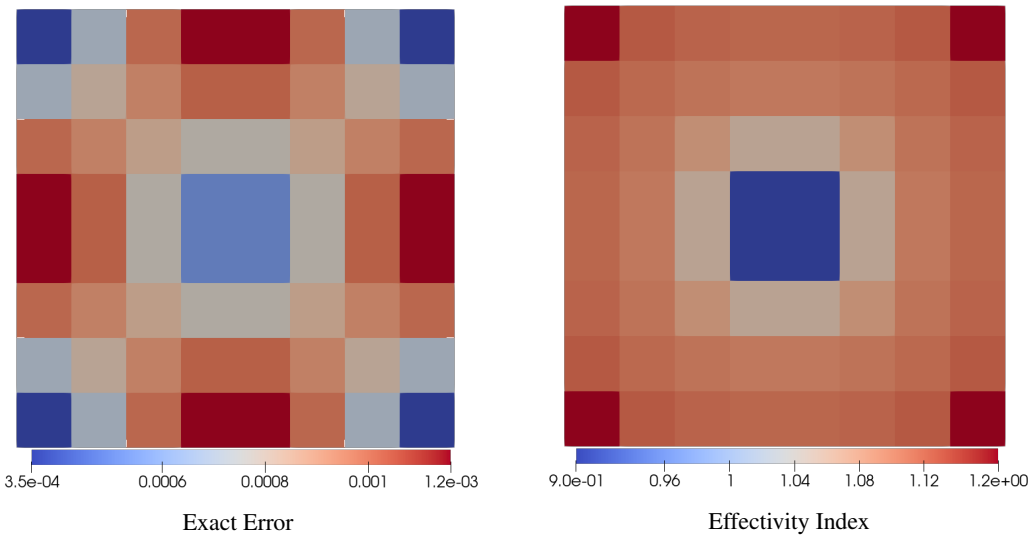

Figure 2. Smooth problem: On the left side, the exact error per element. On the right side, the local effectivity index. The space configuration is $k = 1, n = 3$, and for an element diameter $h = 1/8$.

Problem with singularity: Over the L-shaped domain $\Omega = [-1, -1]^2 \setminus [0, 1] \times [-1, 0]$ we solve (1) with f and g_D being chosen so that the exact solution is the function $u(r,\ \theta) = r^{2/3}\sin(\frac{2}{3}\theta)$, where $r = \sqrt{x^2 + y^2}$ and $\theta = \text{tg}^{-1}(\frac{y}{x})$. The domain is modelled by inserting a single quadrilateral over each quadrant, followed

by uniformly refining them. The simulation is ran by solving the primal hybrid formulation of the problem, where $(u_h, \lambda_h) \in U_k^{+n} \times Y_k$ for $k = 1, n = 3$ are looked for, over the partitions $\mathbb{T} = \{\mathcal{T}_h\}$ such that $h = \{1/4, 1/8, 1/16, 1/32\}$. The progression of the exact and estimated errors are shown on the left side of Fig. 3. The proposed estimated error has been shown to decrease with the same rate as the exact error as the mesh is further refined.

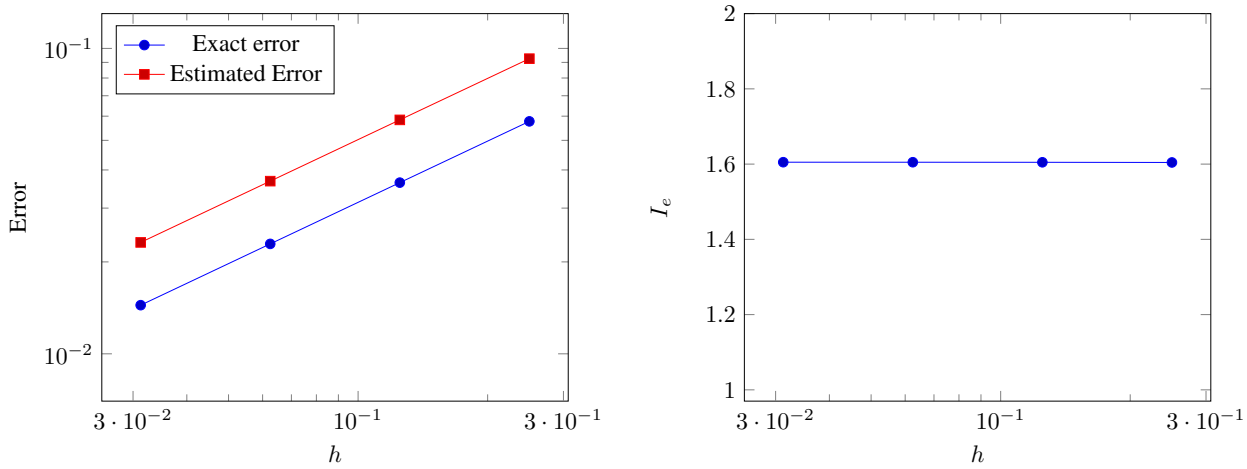

Figure 3. Singularity problem: on the left side, the histories of convergence of the exact error (blue line) and the estimator error (red line). On the right side the effectivity index I_e. The space configuration is $k = 1$, $n = 3$ and $h = \frac{1}{2^j}$, with $j = 1, \cdots 4$.

The errors over each element are shown in Fig. 4, where the exact error per element is shown on the left side and the local effectivity index, on the right. The space configuration is $k = 1, n = 3$ and the element's diameter $h = 1/8$.

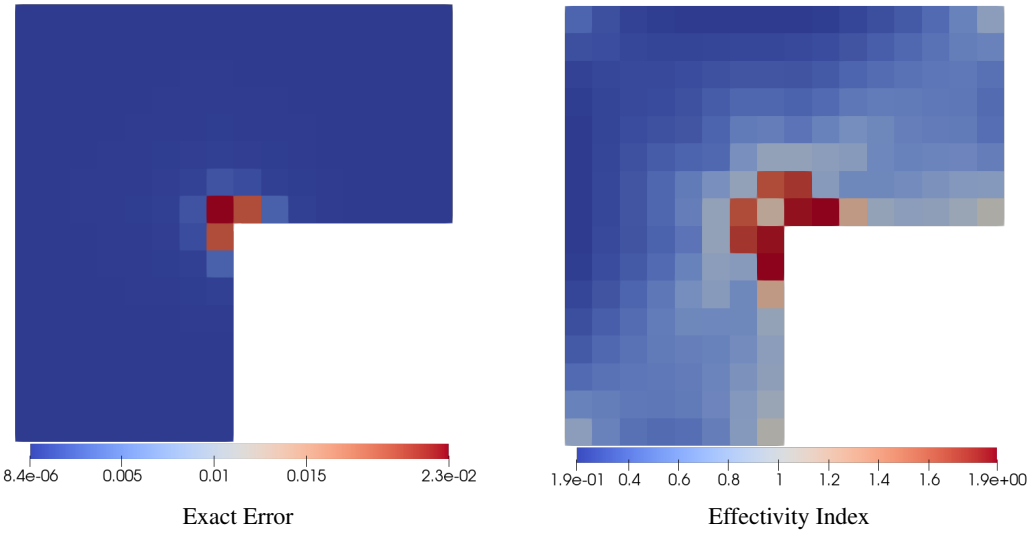

Figure 4. Singularity problem: On the left side, the exact error per element. On the right side, the local effectivity index. The space configuration is $k = 1, n = 3$, and the mesh diameter $h = 1/8$.

The above results illustrate that the estimator captures precisely the behavior of the exact error in both problems. Although, for the singular problem, the upper bound obtained is a little far from the exact error when compared with the analytic case, this is expected if considered the nature of the problem. The numerical results suggests that the estimated error stated in Theorem 1 can be used as an error indicator in an adaptivity process.

5 Conclusion

A new a posteriori error estimation for the primal hybrid finite element method applied to Poisson's equation is proposed. The error estimation is based on the reconstruction of an equilibrated flux and potential, that are obtained by solving local problems which ensures a global smoothing. Numerical examples illustrates the accuracy of the error estimation for a smooth and a singular problems. The results indicates that the strategy is consistent and can be applied to guide adaptive mesh refinement strategies.

Acknowledgements. We gratefully acknowledge the support of EPIC – Energy Production Innovation Center, hosted by the University of Campinas (UNICAMP) and sponsored by Equinor Brazil and FAPESP – Sao Paulo Research Foundation (process 2017/15736-3). We acknowledge the support of ANP (Brazil National Oil, Natural Gas and Biofuels Agency) through the R&D levy regulation. Acknowledgments are extended to the Center for Petroleum Studies (CEPETRO), School of Mechanical Engineering (FEM) and School of Civil Engineering (FEC).

Authorship statement. The authors hereby confirm that they are the sole liable persons responsible for the authorship of this work, and that all material that has been herein included as part of the present paper is either the property (and authorship) of the authors, or has the permission of the owners to be included here.

References

[1] M. Vohralík. Guaranteed and fully robust a posteriori error estimates for conforming discretizations of diffusion problems with discontinuous coefficients. *Journal of Scientific Computing*, vol. 46, pp. 397–438, 2011.
[2] P. R. B. Devloo. PZ: An object oriented environment for scientific programming. *Computer Methods in Applied Mechanics and Engineering*, vol. 150, n. 1-4, pp. 133–153, 1997.
[3] Z. Cai, C. He, and S. Zhang. Generalized prager–synge identity and robust equilibrated error estimators for discontinuous elements. *Journal of Computational and Applied Mathematics*, vol. 398, pp. 113673, 2021.
[4] W. Prager and J. L. Synge. Approximations in elasticity based on the concept of function space. *Quart. Appl. Math.*, vol. , n. 5, pp. 241–269, 1947.
[5] F. Bertrand and D. Boffi. *The Prager–Synge theorem in reconstruction based a posteriori error estimation*, pp. 45–67. American Mathematical Society. KAUST Repository Item: Exported on 2020-10-13, 2020.
[6] D. Braess, V. Pillwein, and J. Schöberl. Equilibrated residual error estimates are p-robust. *Computer Methods in Applied Mechanics and Engineering*, vol. 198, pp. 1189–1197, 2009.
[7] D. Cai, Z. Cai, and S. Zhang. Robust equilibrated error estimator for diffusion problems: Mixed finite elements in two dimensions. *Journal of Scientific Computing*, vol. 83, n. 1. Cited By :2, 2020.
[8] G. V. Pencheva, M. Vohralík, M. F. Wheeler, and T. Wildey. Robust a posteriori error control and adaptivity for multiscale, multinumerics, and mortar coupling. *SIAM Journal on Numerical Analysis*, vol. 51, n. 1, pp. 526–554, 2013.
[9] P. A. Raviart and J. M. Thomas. Primal hybrid finite element methods for 2nd order elliptic equations. *Mathematics of Computation*, vol. 31, pp. 391–413, 1977.
[10] R. Verfürth. *A Posteriori Error Estimation Techniques for Finite Element Methods*. Oxford University Press, 2013.
[11] M. Vohralík. Unified primal formulation-based a priori and a posteriori error analysis of mixed finite element methods. *Math. Comput.*, vol. 79(272), pp. 2001–2032, 2010.
[12] M. Ainsworth and X. Ma. Non-uniform order mixed fem approximation: Implementation, post-processing, computable error bound and adaptivity. *Journal of Computational Physics*, vol. 231, pp. 436–453, 2012.
[13] A. M. Farias, P. R. Devloo, S. M. Gomes, de D. Siqueira, and D. A. Castro. Two dimensional mixed finite element approximations for elliptic problems with enhanced accuracy for the potential and flux divergence. *Computers & Mathematics with Applications*, vol. 74, n. 12, pp. 3283–3295, 2017.